Structure and mechanical properties of liquid crystalline filaments

Alexey Eremin, Alexandru Nemeş, and Ralf Stannarius
Otto-von-Guericke-Universität Magdeburg, FNW/ IEP/ ANP, Postfach 4120, D-39016 Magdeburg, Germany

Mario Schulz
LKA Sachsen-Anhalt, Postfach 180165, D-39028 Magdeburg, Germany

Hajnalka Nádasi and Wolfgang Weissflog
Institut für Physikalische Chemie, Martin-Luther-Universität Halle-Wittenberg, Mühlpforte 1, D-06108 Halle (Saale), Germany
(Received 24 August 2004; revised manuscript received 12 January 2005; published 24 March 2005)

The formation of stable freely suspended filaments is an interesting peculiarity of some liquid crystal phases. So far, little is known about their structure and stability. Similarly to free-standing smectic films, an internal molecular structure of the mesophase stabilizes these macroscopically well-ordered objects with length to diameter ratios of 10^3 and above. In this paper, we report observations of smectic liquid crystal fibers formed by bent-shaped molecules in different mesophases. Our study, employing several experimental techniques, focuses on mechanical and structural aspects of fiber formation such as internal structure, stability, and mechanical and optical properties.

DOI: 10.1103/PhysRevE.71.031705 PACS number(s): 61.30.Hn, 61.10.Nz, 68.37.Ps, 68.65.−k

The formation of free-standing fluid fibers or strands is one of the most striking rheological effects observed in non-Newtonian liquids. Such fibers can be found in nature and technology. For example, spider silk undergoes a mesophase transition in the spinning process, which is considered responsible for the high strength and robustness of that material [1]. Similar fibers appear in several liquid crystalline systems such as polymeric nematics and columnar phases [2–4]. The fibers can be stabilized by the pulling process due to strain hardening, which occurs as a result of the strain dependence of the viscosity [5]. On the other hand, the stability of liquid filaments can also be achieved by an internal molecular layer structure of smectic mesophases. When the smectic layers are wrapped cylindrically around an axial core, such a structure may stabilize a liquid cylinder against the Raleigh-Plateau instability, which in common liquids leads to the rupture of long bridges. However, such a cylindrical layer arrangement is not typical for most of the common smectic phases [smectic-*A* (Sm-*A*), smectic-*C* (Sm-*C*), etc.]. Instead, these materials usually form flat freely suspended films. An exception for smectics is the filament formation in some mixtures like solutions of 8CB in alcohol [6,7]. However, similar Sm-*A* filaments freely suspended in air have not been discovered yet.

One of the most fascinating systems for studying smectic fibers is the liquid crystal mesophases formed by bent-shaped molecules. The transversal anisotropy of such mesogens can considerably hinder the rotations of the molecules around their long molecular axes, favoring polar order. The mesophases formed by such molecules ("banana" or *B* phases) exhibit a variety of interesting phenomena such as spontaneous breaking of chiral symmetry and ferroelectric and antiferroelectric ground states [8,9]. Helical filaments in the isotropic melt [10,11] as well as freely suspended straight fibers [12] have recently been observed in mesophases formed by bent-core compounds. For freely suspended fibers, length to diameter ratios of 1000:1 and more have been reported.

In this work, we study several materials showing polar mesophases (Fig. 1, Table I) with special focus on the structure elucidation of thin freely suspended filaments, their stability, and their mechanical properties.

All mesogens except of compound 5 are fluorinated on the central core and they exhibit a polar smectic-*C* (Sm-CP) phase [13]. In this phase, the molecules are tilted with respect to the layers and the spontaneous polarization vector is perpendicular to the layer normal. In the absence of external electric fields, the layer polarization alternates from layer to layer, resulting in antiferroelectric order. However, even such a simple structure may have several modifications leading to existence of polymorphic variants of the Sm-CP phase [14]. A higher-ordered phase, with an additional in-plane order, is called the B_5 phase (compounds 2, 3, and 4). The mesophases earlier designated by the symbol B_7 show one of the most spectacular microscopic textures.

X-ray studies revealed different structures of the phases exhibiting the same "B_7 texture." Up to date, one can distinguish between at least two different mesophases. The first phase (in this paper B_7) shows several incommensurable x-ray reflections at small and wide angles and, probably, has a complex columnar structure [15]. The second phase is a tilted polar smectic with undulated layers [16]. There are some arguments in favor of existence of a general smectic-*C*

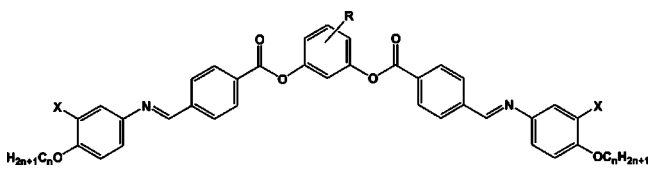

FIG. 1. Chemical formula of the investigated materials (see Table I).

TABLE I. Materials investigated.

No.	*R*	*X*	*n*	Phases and transition temperatures (°C)
1	H	F	10	iso $\overset{160}{\leftrightarrow}$ Sm-*X* $\overset{143}{\leftrightarrow}$ Sm-CP $\overset{90}{\leftrightarrow}$ solid
2	2-CH_3	F	10	iso $\overset{151}{\leftrightarrow}$ Sm-CP[a] $\overset{109}{\leftrightarrow}$ B_5 $\overset{103}{\leftrightarrow}$ solid
3	2-CH_3	F	11	iso $\overset{153}{\leftrightarrow}$ Sm-CP[a] $\overset{114}{\leftrightarrow}$ B_5 $\overset{100}{\leftrightarrow}$ solid
4	5-F	F	9	iso $\overset{154}{\leftrightarrow}$ Sm-CP[a] $\overset{130}{\leftrightarrow}$ B_5[b] $\overset{99}{\leftrightarrow}$ solid
5	2-NO_2	H	16	iso $\overset{172}{\leftrightarrow}$ B_7 $\overset{101}{\leftrightarrow}$ solid

[a]Several polymorphic antiferroelectric smectic-CP phases.
[b]Several polymorphic B_5 phases.

(Sm-C_G) structure of this phase with C_1 symmetry [17–20]. In this phase, there is no in-plane order of the molecules but there exists an out-of-plane component of the spontaneous polarization. The compound designated in Table I as Sm-*X* corresponds exactly to the latter type [19]. However, we would still refrain from the designation Sm-C_G in this paper, until unambiguous evidence for this structure is available.

Our first objective was to test whether filaments could be pulled in the different phases and whether they remain stable. The experiments were performed in a custom-made copper heating box with glass windows; its construction and the observation techniques have been described in [21]. In order to prepare a fiber, a small amount of material is placed on a glass table (Ø 3 mm) inside. Above the table, there is a glass needle which can be moved up and down by means of a stepper motor. In the beginning, the needle tip is dipped into the sample melt. A fiber is drawn by slow pulling of the needle upward. Microscope images of the filaments in transmission are recorded with a digital camera mounted on a Questar QM 100 long range microscope.

It turns out that filaments pulled in the B_7 and Sm-*X* phases represent stable structures; they remain unchanged in the laboratory for days. This is consistent with data reported in the literature [12]. Moreover, in contrast to dynamically stabilized liquid filaments, flow is not required for their stabilization: filaments can be prepared horizontally, in order to exclude continuous material transport between their ends in the gravitational field. Heating the filaments up to the isotropic phase leads to their thinning and rupture (Fig. 2). On the other hand, in the polar Sm-CP phases the compounds form either only unstable filaments or no filaments at all. Depending on the material, these unstable filaments are thinning with progressing time until they eventually rupture. The thinning process may take from some hours to some seconds depending on the compound and the temperature. The loss of stability is particularly interesting in the case of the compound 1 showing a Sm-CP phase *below* the Sm-*X* phase. Not only do the stable filaments in the Sm-*X* phase melt upon the transition into the isotropic phase but they also melt on *cooling* into the Sm-CP phase. It is remarkable that in the latter case the filaments are less stable at lower temperature. There

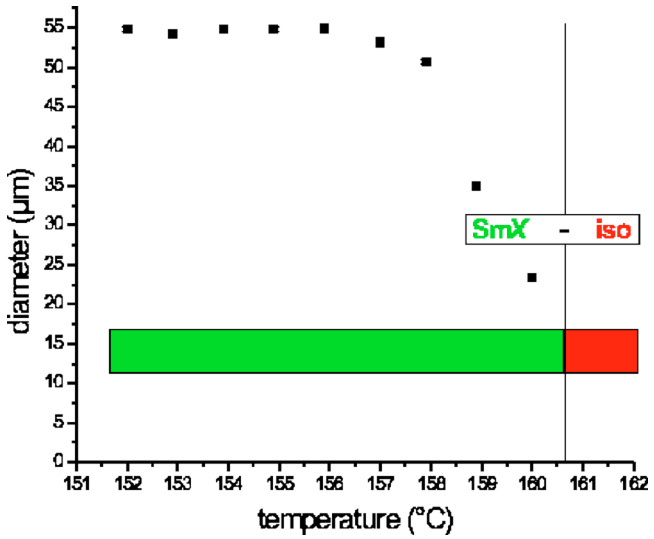

FIG. 2. (Color online) Typical temperature dependence of the filament diameter in the Sm-*X* phase (compound 1). At lower temperatures, the diameter is constant; however, approaching the clearing point, only thinner filaments remain stable.

exists a so far unidentified structural stabilization factor in the higher temperature (less ordered) phase. A speculative explanation is that the higher temperature phase may possess a spontaneous polarization component normal to the layers, which tends to support bent layer structures, while the lower temperature phase possesses an antipolar ordering. The "melting" of a filament during cooling into in the Sm-CP phase is shown in Fig. 3. The pictures show how the surface of the initially uniform vertical filament (a) buckles (b), and molten Sm-CP material flows down (c), leaving a thinner filament (d) that melts soon afterward. The scenario indicates that the filaments are not perfect cylinders but they are often composed of bundles of thinner fibrils (this is investigated in more detail below). The melting of individual fibrils occurs within a few seconds.

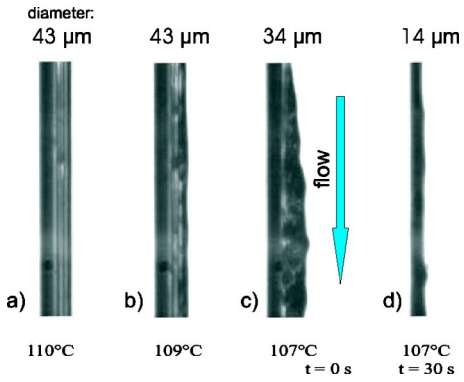

FIG. 3. (Color online) "Melting" of a filament on cooling from Sm-*X* into the Sm-CP phase (compound 1). At temperatures above 110 °C, the diameter of the filament is constant (a). At lower temperatures, its surface starts buckling (b), flow appears, and the filament loses its stability (c). As the flow continues, only a very thin filament remains (d), which melts soon afterward (only a tiny fraction of the filament length is shown).

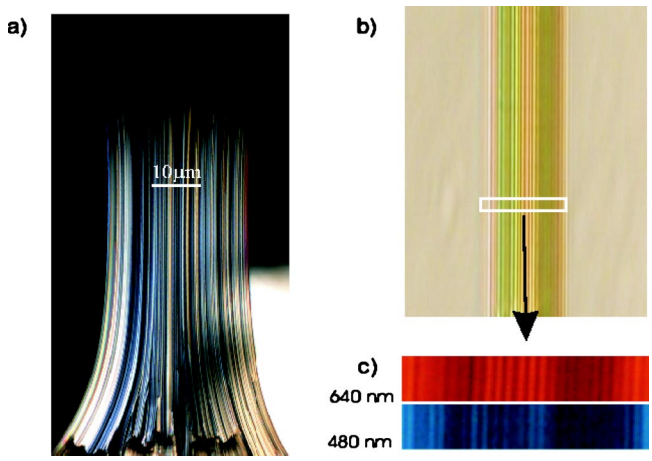

FIG. 4. (Color online) Optical images of fibers: (a) strand composed of thin fibers observed in the reflection polarizing microscope, with crossed polarizers oblique to the filament axis; (b) single filament observed in transmission without polarizers and a fragment of the filament in monochromatic light revealing diffraction stripes parallel to the filament axis; (c) details of (b) observed under monochromatic illumination.

Optically, the filaments are birefringent; they appear black under crossed polarizers parallel and perpendicular to the filament axis. Their optic axis is thus either locally radial, in the plane normal to the filament axis, or axial everywhere. Often, the filaments are clearly identified as bundles composed of thinner fibrils; this is particularly evident in the image of Fig. 4(a). The image has been taken in reflection mode in an optical microscope. The thickness of the structures is independent of the illumination wavelength; the structures have diameters of the order of 1 μm and above. Moreover, one can see the divergence of the bundle at the bottom of the image. These observations show clearly that the filament represents a bundle of separate thin cylindrical structures. However, fine stripe textures along the axes are found on all filaments, irrespective of whether they appear as bundles or single cylinders. Figure 4(b) shows an example of such a filament observed in the long range microscope in transmission. A peculiarity of these fine stripes is that their period depends upon the wavelength λ of the illumination [Figs. 4(b) and 4(c)] in a transmission microscope. The stripes shown in Fig. 4(c) have a periodicity of $(1.88\pm0.1)\lambda$ in the whole visible wavelength range. This indicates that they owe their appearance at least partially to diffraction. A uniform isotropic or optically uniaxial cylinder (e.g., glass) of comparable diameter would show such interference stripes only at the outer edges; therefore we assume that the stripes are due to diffraction effects at longitudinal structures on the surface of the cylindrical filaments. Details of this optical fine structure of filaments are shown in Fig. 5. We emphasize that, although the filaments shown do not have the optical appearance of a uniform cylinder in transmission, they do not represent bundles of filaments in the sense of Jákli *et al.*'s [12] description or like the structures shown in Fig. 4(a). Rather, we consider them as composed of cylinders of tangentially wrapped layers as shown in Fig. 6(b), with the gaps between these cylinders completely filled with more or less ordered smectic material.

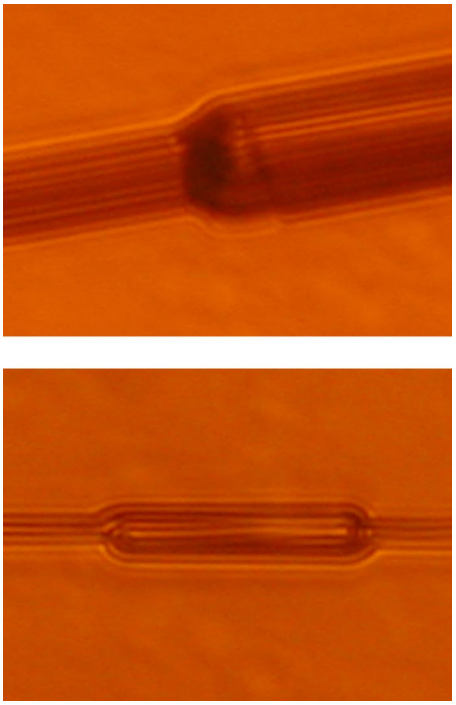

FIG. 5. (Color online) Details of optical images: (a) Filament with a step in diameter from 12.6 to 18.6 μm; (b) filament of 5.85 μm diameter with a bead of diameter 9.6 and length 33.4 μm; the bead grows slowly in length (a few micrometers per minute) by plug flow through the filament.

The existence of the bundle structure can also be supported by atomic force microscopy (AFM) measurements. AFM probes were prepared by rapid cooling of B_7 filaments of compound 5 directly to room temperature where the substance is in a solid (either crystalline or glassy) state. Upon cooling, the optical appearance of the filaments is hardly changed, but they become rigid and brittle. A slight pressure applied to one of the supports breaks them into small pieces which can be studied with AFM. The images in Fig. 6(a) reveal the typical surface modulation along the filament axis. The period of the valleys, which obviously cause the diffrac-

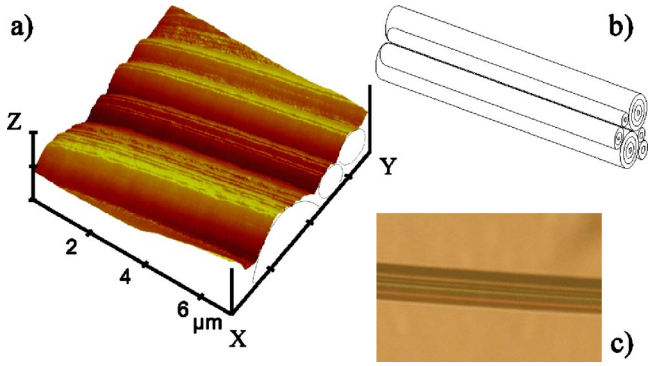

FIG. 6. (Color online) (a) AFM surface profile of a fiber [optical image in (c)] with 50 μm diameter. The surface undulations are parallel to the fiber axis. They suggest that the fibers are formed by bundles of thin cylindrical fibrils of micrometer size, as sketched in (b).

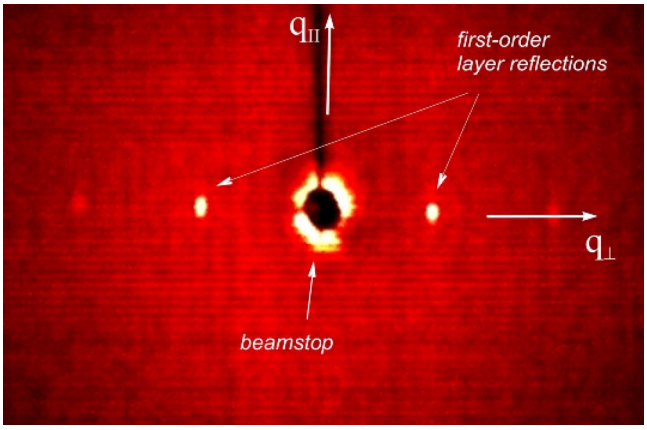

FIG. 7. (Color online) Two-dimensional x-ray pattern of a fiber of compound 1 in the Sm-CP phase, with two layer reflections; the scattering vector is perpendicular to the filament axis. The scattering vector axes $q_{||}$ and $q_{\perp}$ are parallel and perpendicular to the fiber axis. In the Sm-*X* phase, the x-ray pattern is identical.

tion patterns in Fig. 4(a), varies in the range of 0.5–3 μm. This suggests that the cylindrical subunits that form the filaments are in a diameter range of a few micrometers and below. The structural model presented in Fig. 6(b) suggests that single-core filaments are exceptional and may be found particularly in the submicrometer region, whereas all thick filaments observed have a multicore composed structure. The cylindrical shape is developed only on a macroscopic level. This is in contrast to thin planar films or bubbles where the surfaces are flat on both a macroscopic and a microscopic scale.

In order to answer the question how the layers are organized in the fibers, we have performed x-ray scattering measurements in compound 1. Our earlier experiments on powder samples and substrate-oriented droplets [19] showed one single reflection in the small angle region in both Sm-CP and Sm-*X* phases, which corresponds to a layer spacing *d* of 41.8 Å. The incommensurable reflections reported for the B_7 phase in Ref. [15] have not been found in the x-ray patterns of compound 1. Therefore we can draw two conclusions: (1) the Sm-*X* phase is different from the B_7 phases and (2) the Sm-*X* phase has a layer structure. The difference between the Sm-*X* and Sm-CP phases is not quite clear and as already mentioned in Ref. [19], it may lie in the character of the in-plane order of the molecules.

Space-resolved x-ray measurements have been performed on sufficiently thick fibers in both Sm-*X* and Sm-CP phases. In the latter case it was possible irrespective of the limited lifetime of the filament since the fiber was stable for about 1 h at 120 °C. We have used a Cu $K\alpha$ ($\lambda = 1.79$ Å) source in connection with a Hi Star (Siemens AG) two-dimensional area detector. In the x-ray pattern shown in Fig. 7, single-layer reflections are observed. Only the pattern of the Sm-CP phases is shown here since the x-ray pattern of the filament in the Sm-*X* phase (at 150 °C) is identical. In agreement with our previous studies, the layer spacing hardly depends on temperature. The scattering vector of the layer reflections is perpendicular to the fiber surface, which indicates (assuming that all directions normal to the filament axis are equivalent)

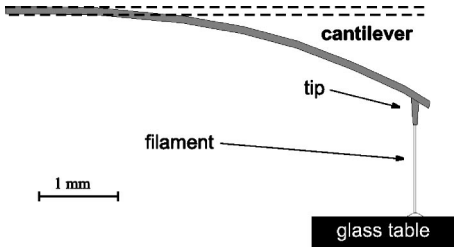

FIG. 8. Setup for tension measurements of liquid filaments.

that the smectic layers are indeed wrapped into coaxial cylinders. The layer thickness in the fibers remains the same as in the bulk. Interestingly, the correlation length estimated from the width of the first reflection (full width at half maximum) is larger in the fiber than in bulk ($\xi_{\text{bulk}} \approx 4100$ Å and $\xi_{\text{fiber}} \approx 4850$ Å). This implies that the degree of smectic order in the filaments is higher than in the bulk material. Irrespective of the existence of a smectic layer structure, the material is liquid within the layers. Upon cooling into the solid state we have not observed any considerable change in the peak width, but the fluidity completely disappears.

One of the interesting questions that arise is the mechanical characterization of the filaments. We have constructed a setup for the measurement of the axial stress exerted by such structures. The tension in the filaments is determined with the help of a cantilever (Fig. 8) that allows, in principle, static and dynamic measurements.

The cantilever consists of a thin 8 μm gold plate with a small tip (0.8 mm length, 80 μm diameter) at the end (Fig. 8). The deflection of the plate is recorded as a measure of the force excerted by the filament. It was gauged before the measurement with the help of a small weight attached to the cantilever tip. The very small force constant, the product of the Young modulus *E* and the inertia moment *I*, $EI = 0.46 \times 10^{-5}$ N, provides sufficiently high sensitivity in the range of micronewtons. The measured force exerted by a 15 μm thick filament of fixed length has been determined as 12×10^{-7} N. Assuming in first approximation that the filament has a perfect cylindrical shape, the surface energy E_s can be expressed by the radius *r*, the length *l*, and the surface tension γ: $E_s = 2\pi r l \gamma$. This formula allows us to estimate the surface tension from measurements of the stress $T = dE_s/dl = 2\pi r \gamma$ exerted by a cylindrical filament. Gravitational forces can be completely neglected. The values obtained for several samples with different radii in the experiments yield an apparent surface tension $\gamma = 26 \pm 2$ mN/m for compound 1 ($T = 155$ °C). These figures comply satisfactorily with values of the surface tension in conventional smectics; actually the result is slightly higher than one might expect from the chemical structure [22]. Additionally, our results obtained by the cantilever method are in good agreement with the data from resonant measurements reported by Jákli *et al.* [12]. Probably, the value is overestimated by 20–30 % by the approximations, since we have assumed a smooth, cylindrical surface, whereas the actual surface is corrugated as seen in the AFM images (Fig. 6). Taking this into consideration, the stress measurements fully corroborate our assumption of a compact filament structure where surface tension plays a dominant role. Further experiments should be devoted to the

determination of the apparent dynamic surface tension during the pulling of the filaments.

Summarizing, a number of experiments characterizing free-standing liquid filaments of different mesophases have been presented. Clearly, the experiments show that there is a concurrence between free-standing fibers and free-standing films in the investigated mesophases. So far, it is not fully understood which mesophase structures belong to the class of filament-forming phases. The existence of a smectic layer structure alone proves to be not sufficient. In particular, the x-ray measurements of compound 1 show that the geometrical structures of two phases of the same material can be practically identical whereas filaments are stable in one of these mesophases and unstable in the other (lower temperature) mesophase. Very high values of the macroscopic polarization in the smectic phases formed by the bent-shaped molecules may contribute to the high anisotropy of the surface tension. Probably, a spontaneous curvature of the layers, which might be caused by an out-of-plane component of the polarization [12,17], favors the formation of cylindrical fibers rather than free-standing flat films. This would explain why existing filament structures are destroyed when the samples are cooled or heated into Sm-CP mesophases in which the layer structure is still present.

The authors acknowledge very greatly I. Grodrian and L. Naji for their AFM measurements. The DFG is acknowledged for financial support within Project No. STA 425/15.

[1] F. Vollrath and D. P. Knight, Nature (London) **410**, 541 (2001).
[2] A.-G. Cheong, A. D. Rey, and P. T. Mather, Phys. Rev. E **64**, 041701 (2001).
[3] D. H. Van Winkle and N. A. Clark, Phys. Rev. Lett. **48**, 1407 (1982).
[4] D. M. Walba, L. Xiao, P. Keller, R. Shao, D. Link, and N. A. Clark, Pure Appl. Chem. **71**, 2117 (1999).
[5] M. Reine, Phys. Today **17**(1), 62 (1964).
[6] M. Todorokihara, H. Naito, and O. Y. Zhong-Can, Mol. Cryst. Liq. Cryst. Sci. Technol., Sect. A **328**, 549 (1999).
[7] H. Naito, M. Okuda, and Ou-Yang Zhong-can, Phys. Rev. Lett. **70**, 2912 (1993).
[8] T. Niori, T. Sekine, J. Watanabe, T. Furukawa, and H. Takezoe, J. Mater. Chem. **6**, 1231 (1996).
[9] D. R. Link, G. Natale, R. Shao, J. E. Maclennan, N. A. Clark, E. Körblova, and D. M. Walba, Science **278**, 1924 (1997).
[10] G. Pelzl, S. Diele, A. Jákli, CH. Lischka, I. Wirth, and W. Weissflog, Liq. Cryst. **26**, 135 (1999).
[11] A. Jákli, CH. Lischka, W. Weissflog, G. Pelzl, and A. Saupe, Liq. Cryst. **27**, 1405 (2000).
[12] A. Jákli, D. Krüerke, and G. G. Nair, Phys. Rev. E **67**, 051702 (2003).
[13] H. Nádasi, Ph.D. thesis, Martin-Luther University, Halle, 2004.
[14] A. Eremin, I. Wirth, S. Diele, G. Pelzl, H. Schmalfuss, H. Kresse, H. Nádasi, K. Fodor-Csorba, E. Gács-Baitz, and W. Weissflog, Liq. Cryst. **29**, 775 (2002).
[15] G. Pelzl, S. Diele, and W. Weissflog, Adv. Mater. (Weinheim, Ger.) **11**, 707 (1999).
[16] D. A. Coleman, J. Fernsler, N. Chattham, M. Nakata, Y. Takanishi, E. Körblova, D. R. Link, R.-F. Shao, W. G. Jang, J. E. Maclennan, O. Mondainn-Monval, C. Boyer, W. Weissflog, G. Pelzl, L.-C. Chien, J. Zasadzinski, J. Watanabe, D. M. Walba, H. Takezoe, and N. A. Clark, Science **301**, 1204 (2003).
[17] A. Jákli, D. Krüerke, H. Sawade, and G. Heppke, Phys. Rev. Lett. **86**, 5715 (2001).
[18] A. Jákli, G. G. Nair, H. Sawade, and G. Heppke, Liq. Cryst. **30**, 265 (2003).
[19] A. Eremin, S. Diele, G. Pelzl, H. Nádasi, and W. Weissflog, Phys. Rev. E **67**, 021702 (2003).
[20] J. P. Bedel, J. C. Rouillon, J. P. Marcerou, H. T. Nguyen, and M. F. Achard, Phys. Rev. E **69**, 061702 (2004).
[21] H. Schüring, R. Stannarius, C. Tolksdorf, and R. Zentel, Macromolecules **34**, 3962 (2001).
[22] P. Mach *et al.*, Langmuir **14**, 4330 (1998).